Proc. Nat. Acad. Sci. USA
Vol. 71, No. 5, pp. 1672–1676, May 1974

X-Ray Diffraction Studies of Nucleohistone: A Polyhelical Model of Chromosome Organization

(DNA/chromatin/lampbrush organization)

JUAN A. SUBIRANA AND LUIS C. PUIGJANER

Departamento de Química Macromolecular del C.S.I.C., Universidad Politécnica, Diagonal 999, Barcelona-14, Spain

Communicated by Paul Doty, January 21, 1974

ABSTRACT **The possibility that nucleohistone is constituted by a helical arrangement of DNA molecules is analyzed in this paper. A polyhelical model of nucleohistone in plectanemic double coils of variable dimensions is found to be compatible with the x-ray diffraction results obtained in this and other laboratories. The radius of the coils varies between 35 and 45 Å, whereas the pitch varies between 200 and 120 Å. Another part of nucleohistone is much less coiled and contributes to the "background" scattering of the sample. This model is compatible with a lampbrush organization of the chromosome.**

Several models have been proposed for the structure of nucleohistone on the basis of x-ray diffraction studies. Thus, Bram and Ris (1) have suggested that in dilute solution it is made of an irregular coil with a radius of gyration of about 30 Å. In more concentrated systems it has been known for some time (2, 3) that nucleohistone acquires a more ordered conformation, characterized by a series of diffraction rings which have been interpreted to arise either from intermolecular packing (3) or from the intramolecular nucleohistone conformation (4, 5). More recently new x-ray diffraction studies have been published (6, 7) which show that the position and relative intensity of the diffraction rings may vary depending on the conditions used to prepare the samples. In this paper we show that these results can be interpreted on the basis of a polyhelical model of nucleohistone structure.

MATERIALS AND METHODS

Preparation of Nucleohistone. Nucleohistone from calf thymus was prepared as described elsewhere (8). In essence, the method consists in purifying the nuclei by successive resuspension in the following reagents: (*1*) 0.25 M sucrose, 3 mM $CaCl_2$; (*2*) 2 M sucrose, 3 mM $CaCl_2$, 0.5% Triton X-100; (*3*) 0.1 M Tris·HCl, pH 8, twice; (*4*) 0.15 M NaCl. The purified nuclei obtained in this way are resuspended and sheared in 1 mM ethylenediaminetetraacetic acid (EDTA), 1 mM sodium cacodylate, pH 8. Fibers were pulled from the precipitate obtained after mixing the nucleohistone suspension with an equal volume of 0.25 M NaCl.

X-ray Diffraction Studies. Fibers were placed in sealed capillaries which contained a drop of saturated salt solution to maintain a constant relative humidity. Diagrams were obtained either with a Statton pinhole camera (specimen to film distance 7 cm) and an Enraf fine focus generator or with a commercial toroidal camera (Baird and Tatlock) and an AMR-Norelco microfocus generator.

Mathematical Model. The model used by Franklin and Klug (9) in their studies of tobacco mosaic virus (TMV) was adapted to the present problem. The axis of each DNA molecule was assumed to follow a helix (which we will call coil to distinguish it from the DNA double helix) of radius δ and pitch p. The ratio p/δ will be called z. Two DNA molecules were assumed to be wound into a plectanemic double coil. The cross-section of each DNA molecule by a plane perpendicular to the axis of the coil was assumed to be a circle of radius 10 Å. The angle formed by the lines which go from the center of each DNA molecule to the axis of the coil in a cross-section was called α. The cylindrically averaged transform of such a model placed perpendicular to the x-ray beam can be calculated as described by Franklin and Klug (9). Under the assumption that the molecules are infinitely long, the transform of a fully disordered system of such coils can be obtained simply by superposing the diffraction at all points in two-dimensional reciprocal space, divided by the distance to the center of coordinates in reciprocal space. This was shown quite generally by Porod (10). The intensity is, therefore, calculated by the following expression:

$$I(R) = (A_{01} + A_{02})^2/R + 2\sum_{n=1}^{n=n_{max}} (A_{n1}^2 + A_{n2}^2 + 2A_{n1}A_{n2}\cos n\alpha)/R \quad [1]$$

where

$$A_{n1} = J_n(2\pi\delta_1 R')\pi r_1^2 \frac{2J_1(2\pi R' r_1)}{2\pi R' r_1} \quad [2]$$

$$A_{n2} = J_n(2\pi\delta_2 R')\ \pi r_2^2 \frac{2J_1(2\pi R' r_2)}{2\pi R' r_2} \quad [3]$$

$$R' = \{R^2 - (n/p)^2\}^{1/2}. \quad [4]$$

In these expressions n is the layer line number, J_ns are the Bessel functions of order n, and R is the reciprocal space coordinate, equivalent to the abscissa in the intensity plots given below. The expression *1* is valid up to a value of R given by $R_{max} = n_{max}/p$. The calculations were usually carried out for $R_{max} = 0.06$. The cross sections of the coils by a plane perpendicular to their common axis are circles of radii r_1 and r_2. In most calculations, $r_1 = r_2 = 10$ Å, and $\delta_1 = \delta_2 = \delta$, the radius of the coils. However, in Fig. 1*D*, δ_1 was equal to zero and the value of r_1 was adjusted so that the mass per unit length of both components of the coil was the same.

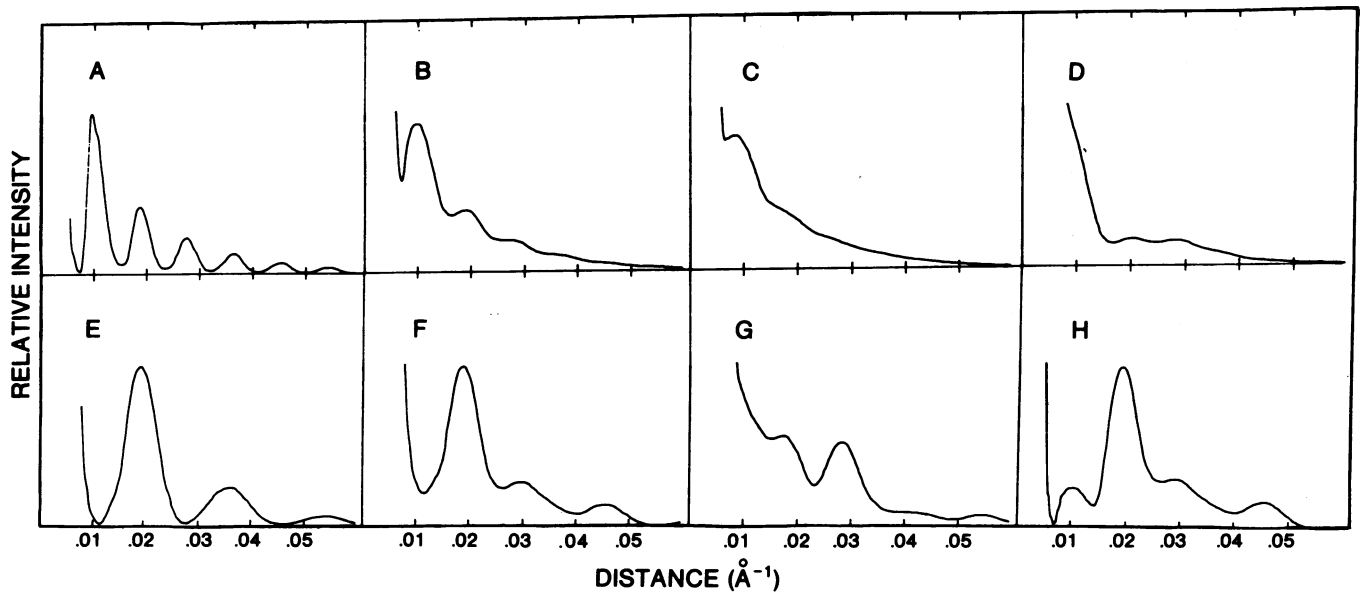

FIG. 1. Theoretically computed diffraction patterns of disordered systems of infinitely long regular coils. In all cases, the cross-section of each coil by a plane perpendicular to its axis is a circle of 10-Å radius. Other parameters are the following: (*A*) single coil with radius δ = 50 Å and pitch p = 120 Å; (*B*) single coil with δ = 34 Å and p = 136 Å; (*C*) single coil with δ = 30 Å and p = 150 Å. Comparison of these three patterns shows that when the value p/δ increases, the layer-line peaks broaden and become superimposed, so that they can no longer be distinguished; (*D*) single coil with δ = 34 Å and p = 136 Å. In this case, an additional DNA molecule, represented by a cylinder of 10-Å radius and adequate density, is present in the axis of the coil. The structure is similar to a double coil, in which one of the coils is straight (δ = 0) and the other is wound around it; (*E*) double coil with δ = 34 Å, p = 136 Å, α = 180°. In this case, since the structure is symmetrical, the peaks due to odd layer lines disappear; (*F*) *ibidem*, with α = 150°; (*G*) *ibidem*, with α = 120°. Comparison of these three patterns shows the large influence of α on the contribution of each layer line. The individual peaks are more distinct than in the pattern shown in *B* (α = 0°). (*H*) double coils with δ = 34 Å, p = 136 Å, α = 150°. In this case the interaction between groups of coils is taken into account as described by Oster and Riley (12). Groups of seven coils in an hexagonal arrangement are considered. The distance between coil axes is 60 Å.

A Hewlett–Packard 2116B Computer provided with a plotting attachment was used for the calculations. Bessel functions were obtained from an algorithm using a relative error correction term better than 10^{-4}. The details of the mathematical model and computations will be presented elsewhere (11).

Catgut Model Experiments. Circular structures of catgut threads (0.6-mm diameter, kindly provided by Laboratorios Arago, Barcelona) were made by tying together several pieces. Coiling of these structures was induced by heating the threads immersed in water.

RESULTS

X-ray Diffraction Patterns. The patterns obtained from calf-thymus nucleohistone show the typical rings and 30-Å equatorial spot described by Wilkins and collaborators (2). The positions of the rings obtained with several samples are given in Table 1. A microdensitometer tracing is shown in Fig. 3. Although the positions of the rings obtained by us approximately coincide with those reported by other investigators (2, 3, 5–7), their relative intensities apparently depend on the conditions of preparation of the sample (7).

Model Calculations. Some of the theoretical scattering curves obtained with the model presented above are shown in Fig. 1. A more detailed discussion will be presented elsewhere (11). The diagrams shown illustrate the most prominent features of the behavior of disordered coils. The curves *A–C* demonstrate that when the parameter z (pitch/radius) increases, the peaks tend to overlap. For z greater than 5, only the first peak can be distinguished in single coils. On the other hand, when z has the value 2 or smaller, additional peaks appear due to equatorial maxima. The influence of the relative position of the two DNA molecules which form the coil is illustrated with the curves *E–G*. When the two molecules are diametrically opposed (α = 180°), only the peaks due to even layer lines can be detected (Fig. 1*E*). For other values of α, other peaks appear, the intensity of which depends strongly on the precise value of α. The peak due to the first layer line is hidden in the central equatorial maximum for α greater than about 100°. The exact value depends on z.

The curves shown demonstrate that the degree of overlap intensity of the different peaks depend strongly on α and z. On the other hand, a striking property of the scattering curves is that the relative position of the maxima is practically independent of pitch and radius and only depends slightly on α. Some typical values are given in Table 1. Thus, for α = 0° (single coil), if the first layer line maximum occurs at 100 Å, the next higher order maxima always appear at about 53, 36, and 28 Å, respectively. The parameters of the coils which have the same position of maxima are given in Fig. 2.

Two additional scattering curves are shown in Fig. 1. Curve *H* shows the behavior of a group of coils packed in a partially regular manner. In this case, the first layer line peak can be clearly detected due to the decreased intensity of the central equatorial peak. Curve *D* shows an opposite effect, given by a model in which a DNA molecule is wound in the form of a coil around another straight DNA molecule which follows the axis of the coil. In this case the central scattering increases so that the layer-line peaks are barely detectable.

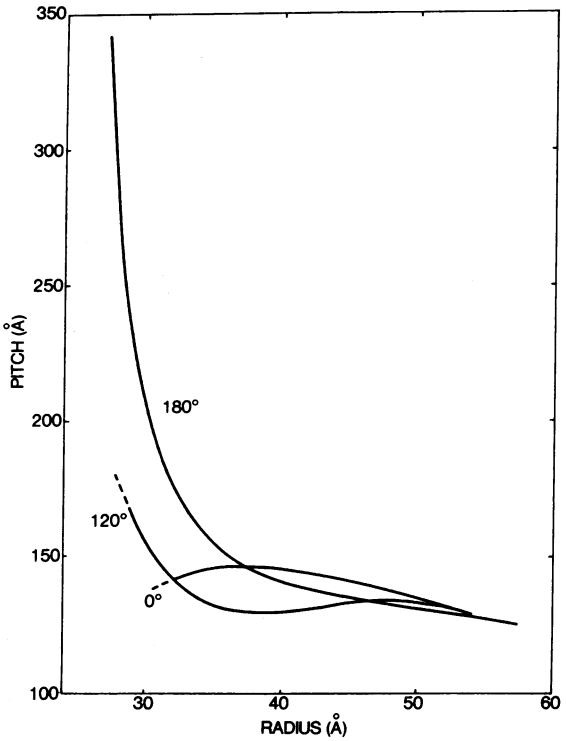

FIG. 2. Dimensions of the coils which show a second order peak at 0.178 reciprocal Å (1/56.2 Å). The diagram is not continued to higher values of δ because in this region the equatorial peaks become prominent and appear together with the layer line peaks, a situation which is not experimentally observed. For low values of δ, the 0° and 120° curves cannot be continued because the peaks become superimposed and cannot be distinguished in the continuously decreasing scattering curve. For 180°, a peak is detected in this area, although it is due to an equatorial reflection which gradually dominates the second order peak.

Comparison with the Experimental Curves. From the calculations presented it is clear that the experimental calf-thymus curve cannot be described by a single coil of uniform dimensions. The ratio of the positions of the second and third layer-line peaks in a single coil has been calculated to be 0.69 (Table 1). When the parameters of the coil (either pitch or radius) are allowed to change, this ratio changes less than 0.01 about its average value 0.69. On the other hand, the experimental value of this ratio in different calf-thymus samples studied in our laboratory has been found to be about 0.62 (Table 1). This value coincides with the average of values reported by Olins and Olins (6), whereas Bradbury *et al.* (7) have found even smaller values of this ratio. This discrepancy is well beyond the limits of experimental error, so that it does not appear possible to use a single coil to take into account the results obtained. The position of the peaks has also been found to vary significantly in different samples (6, 7). Furthermore, there are some features of the scattering curves which are best interpreted with a model based on a double coil. These include the small relative intensity of the first layer-line peak (13) and the variability of the 27-Å fourth layer-line peak under different conditions (7).

In order to reproduce the experimental calf-thymus curve by a theoretical model, the major difficulty lies in the fact that there is a whole family of coils which give the same position of the major peak, at about 57 Å as shown in Fig. 2. This uncertainty can be partially removed if it is assumed that nucleohistone in fibers will have an average radius of gyration close to 30 Å, as determined by Bram and Ris (1) in dilute solution. Fig. 3 shows a theoretical curve (broken line) obtained by the addition of the scattering of three different coils, one of which is mainly responsible for the "background" scattering (δ = 15, p = 275, α = 180°) and the other two for the layer line peaks (δ = 36, p = 180, α = 150° and δ = 42, p = 126, α = 150°). This choice of particular coils is certainly not unique, but indicates the order of magnitude of the dimensions of the coils which are required to interpret the calf-thymus nucleohistone pattern. No assumption is made about the handedness of the coils. A mixture of left and right handed coils might be present. The choice in the dimensions given is based on the assumption that there will be certain rules which limit the variability of the nucleohistone coils. If histones bind the two DNA component strands which form a double coil, a logical rule is that the length of DNA in a coil pitch will be constant ($p^2 + (2\pi\delta)^2$ = constant). This rule is obeyed by the three coils involved in the theoretical curve shown in Fig. 2. It means that we can transform one of the coils into another

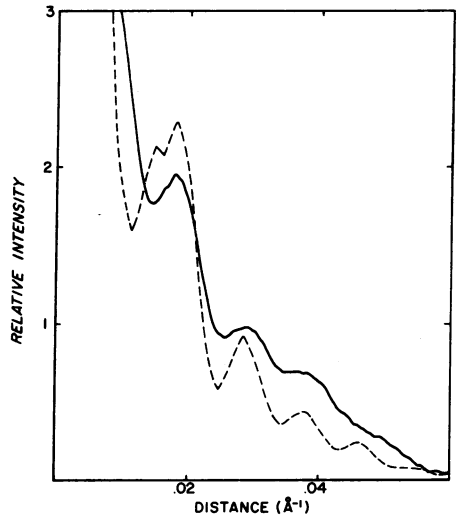

FIG. 3. Comparison of an experimental and a computed diffraction pattern. The experimental curve (continuous line) is a microdensitometer tracing along the meridional direction of a pattern obtained from calf-thymus nucleohistone at 97% relative humidity. Instrumental scattering has not been corrected. It is only appreciable below 0.015 Å^{-1}. The computed pattern (broken line) is obtained by the addition of three component coils: δ = 15, p = 275, α = 180°; δ = 36, p = 180, α = 150° and δ = 42, p = 126, α = 150°. These coils are added in relative proportions which respectively are 16%, 42%, and 42%. The position of the peaks coincides exactly in both the experimental and theoretical curve. The percentages taken of each component do not alter much this result. The 57-Å peak appears split in the theoretical curve, due to the fact that the two latter coils contribute to this peak. However, this behavior should not be experimentally observed, since the real dimensions of the coils will vary continuously between the values given. Agreement in the intensity of each peak with the experimental results could be improved by adding more coils of intermediate dimensions, taking into account the packing interaction between coils (Fig. 1*H*) and introducing a contribution from rope-like structures and coils of the type shown in Fig. 1*D*. The fact that the nucleohistone coils are not infinitely long would produce a flattening of the maxima observed.

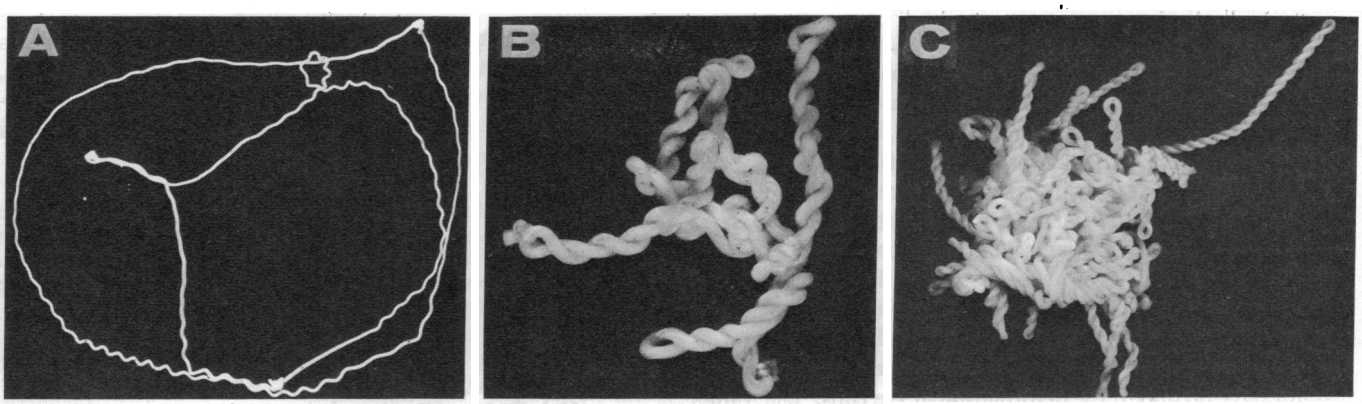

FIG. 4. Shapes taken by catgut threads allowed to coil: (*A*) three 60-cm pieces circularly attached end to end photographed in an intermediate stage. Single-coil regions appear which are unstable, they later disappear at the end of the process; (*B*) the same thread photographed at the end of the coiling process. Double coils are prominent. Quadruple coils are also present; (*C*) structure obtained from a 12-m circular structure. Double coils are the most prominent feature, although quadruple coils and more complex rope-like structures are also present. Experiments carried out with other thread materials gave similar results, although in some cases (polyethylene threads) the coils obtained were wound in a much looser fashion.

simply by longitudinal deformation along the axis of the coil, in other words, the number of turns of the coil remains constant for a given length of DNA. Furthermore, the distance across the major groove of the third coil is similar to the distance between the two DNA strands in the second coil, a fact which should be expected if this distance is covered by histone bridges.

The values chosen for α must also be considered. In a double coil formed by two equal DNA helices, a symmetrical arrangement should be expected, in other words, α should be 180°. However, if histones are not arranged symmetrically with regard to the two DNA helices, the value of α may change. As a matter of fact, in order to take into account the experimental results, α cannot be 180° for all component coils, since the peaks due to odd layer lines would then disappear. Diminishing α to about 150° is sufficient to give rise to a well developed peak at about 36 Å as shown in Fig. 3. It appears, therefore, that the distribution of histones is not symmetric with regard to the DNA helices involved in the formation of the double coil.

It should be noted that, although the experimentally measured spacings change, they do so only to a limited extent. A much larger variability would be apparently expected, if the dimensions of the coils which constitute nucleohistone vary. However, the constraints imposed by the presence of histones reduce this variability to narrow limits so that the spacings actually measured do not change much. In isolated nuclei, a much higher central scattering is observed, so that the 55-Å spacings cannot be measured. This behavior can be taken into account by increasing the relative amount of the most stretched coil ($p = 275, \delta = 15$).

TABLE 1. *Calculated parameters for single coils and experimental parameters for nucleohistone*

Radius	Pitch	L_2	L_3	L_4	L_3/L_2	L_4/L_2
50	120	52.4	36.0	27.2	0.69	0.52
34	136	51.1	36.2	28.0	0.69	0.54
30	150	Not detectable			—	—
Experimental		56.0	35.7	26.3	0.64	0.47
		57.5	35.3	27.0	0.61	0.47
		57.0	35.5	26.4	0.62	0.46
		57.7	35.2	27.8	0.61	0.48

All dimensions and spacings are given in Ångströms. L_i represent the spacings due to the i ring in the measured or calculated patterns. The experimental values correspond to calf-thymus nucleohistone fibers equilibrated to 97% relative humidity.

Another feature of interest of the choice of coils made is that upon partial orientation of the sample in a fiber one would expect that the most elongated coil would be the one best oriented, in this case the coil of 15-Å radius. Under these conditions of orientation, this coil would give rise to an equatorial peak at 30-Å spacing, as it is usually observed in fibers. It is likely that upon extensive elongation the pitch of this coil will increase, so that the DNA molecules will tend to align themselves parallel to the direction of elongation. Uncoiled molecules, packed parallel to the axis of the fiber, will also contribute to the 30-Å spacing.

A Polyhelical Model of Chromatin Structure. As shown in the previous paragraph, the experimental scattering curves can be interpreted according to a model which involves coils of different dimensions. For a better understanding of the mechanics of coil formation, we carried out some model experiments with catgut threads which are shown in Fig. 4. It is apparent from this figure that under the influence of torsional forces a long thread can be packed into a small volume. The most prominent structures which appear are double coils, although quadruple and more complex coils are also observed. The latter types of coils mainly reinforce the 27-Å peak, which under some conditions is found to be very strong (7). In intermediate states single coils appear as unstable structures. With other materials it is also possible to observe structures in which a straight thread is surrounded by a coiled thread. The x-ray diffraction results and these model experiments suggest that chromatin may be organized in polyhelical structures of this type. This arrangement would also explain the limited orientation of nucleohistone fibers. This model leads to a lampbrush model of chromosome structure as a logical consequence. The typical changes of chromatin condensation during mitosis might be explained by a modification in the degree of coiling induced by changes in the ionic or chemical environment of chromatin.

DISCUSSION

The model presented allows an interpretation of the variations in the x-ray diffraction pattern reported for different samples of chromatin (1–7). It has some features in common with those suggested by other authors (3–5, 14). In the present model changes in the coil parameters are allowed. These changes may be due to local differences in the histone to DNA ratio, perhaps related to the local base sequence of the DNA.

The scattering curve of nucleohistone in dilute solution (1) can also be interpreted according to the model presented here, if it is assumed that the nucleohistone coils have a certain amount of flexibility in solution, so that the layer line peaks cannot develop due to the deformation of the coils. The value of 30 Å determined for the radius of gyration of nucleohistone under these conditions (1) may represent the average of the different coiled regions present.

Comparison of the model presented with electron microscopy results is difficult, since a limitation of this method lies in the fact that the samples must be observed in the dry state, often after a chemical treatment of the chromatin which does not warrant a preservation of its native structure. The 100-Å fibers frequently reported (1) may either correspond to collapsed double coils or to stretched and later collapsed single coils. The presence of lateral extensions in these fibers is likely due to short double coils, in a way similar to the models shown in Fig. 4.

Finally, it must be stressed that although this model explains most of the features of x-ray scattering by chromatin, other models based on a folded structure can equally well be used to interpret the scattering curves of nucleohistone. Ways of folding can be devised, with periods similar to the pitch of the coils used here, which give rise to scattering curves very similar to those given by a group of coils. Another possibility, analyzed in detail elsewhere (15), is that the diffraction rings are due to a partially regular distribution of histones along the DNA with a periodicity close to 110 Å. However, until more relevant experimental data are available, a polyhelical model allows a simple explanation of the results presently known.

We are thankful to Mr. J. Cortadas and Miss G. Rocamora who prepared the catgut models and to Mr. P. Suau for his help in obtaining the diffraction patterns shown in Fig. 3 and Table 1. This research was supported by a grant from The Population Council, New York.

1. Bram, S. & Ris, H. (1971) *J. Mol. Biol.* **55**, 325–336.
2. Wilkins, M. H. F., Zubay, H. & Wilson, H. R. (1959) *J. Mol. Biol.* **1**, 179–185.
3. Luzzatti, V. & Nicolaieff (1963) *J. Mol. Biol.* **7**, 142–163.
4. Pardon, J. F., Wilkins, M. H. F. & Richards, B. M. (1967) *Nature* **215**, 508.
5. Pardon, J. F. & Wilkins, M. H. F. (1972) *J. Mol. Biol.* **68**, 115–124.
6. Olins, D. E. & Olins, A. L. (1972) *J. Cell Biol.* **53**, 715–736.
7. Bradbury, E. M., Molgaard, H. V., Stephens, R. M., Bolund, L. A. & Johns, E. W. (1972) *Eur. J. Biochem.* **31**, 474–482.
8. Subirana, J. A. (1973) *J. Mol. Biol.* **74**, 363–386.
9. Franklin, R. & Klug, A. (1956) *Biochim. Biophys. Acta* **19**, 403–416.
10. Porod, J. (1948) *Acta Phys. Austr.* **2**, 255–292.
11. Puigjaner, L. C. & Subirana, J. A. (1974) *J. Appl. Crystallogr.* **7**, in press.
12. Oster, G. & Riley, D. P. (1952) *Acta Crystallogr.* **5**, 272–296.
13. Pardon, J. F. & Richards, B. M. (1972) *Chromosomes Today* **3**, 38–46.
14. Sorsa, V. & Sorsa, M. (1967) *Ann. Acad. Sci. Fenn. Ser.* A,IV **105**, 1–18.
15. Subirana, J. A., Puigjaner, L. C., Roca, J., Llopis, R. & Suau, P. (1974) in *The Structure and Function of Chromatin*, ed. Wolstenholme, G. E. W. (Associated Scientific Publishers, Amsterdam), in press.